

Search for Dark Photons Produced in 13 TeV pp CollisionsR. Aaij *et al.**
(LHCb Collaboration) (Received 15 December 2017; published 8 February 2018)

Searches are performed for both promptlike and long-lived dark photons, A' , produced in proton-proton collisions at a center-of-mass energy of 13 TeV, using $A' \rightarrow \mu^+\mu^-$ decays and a data sample corresponding to an integrated luminosity of 1.6 fb^{-1} collected with the LHCb detector. The promptlike A' search covers the mass range from near the dimuon threshold up to 70 GeV, while the long-lived A' search is restricted to the low-mass region $214 < m(A') < 350 \text{ MeV}$. No evidence for a signal is found, and 90% confidence level exclusion limits are placed on the γ - A' kinetic-mixing strength. The constraints placed on promptlike dark photons are the most stringent to date for the mass range $10.6 < m(A') < 70 \text{ GeV}$, and are comparable to the best existing limits for $m(A') < 0.5 \text{ GeV}$. The search for long-lived dark photons is the first to achieve sensitivity using a displaced-vertex signature.

DOI: 10.1103/PhysRevLett.120.061801

The possibility that dark matter particles may interact via unknown forces, felt only feebly by Standard Model (SM) particles, has motivated substantial effort to search for dark-sector forces (see Ref. [1] for a review). A compelling dark-force scenario involves a massive *dark photon*, A' , whose coupling to the electromagnetic current is suppressed relative to that of the ordinary photon, γ , by a factor of ϵ . In the minimal model, the dark photon does not couple directly to charged SM particles; however, a coupling may arise via kinetic mixing between the SM hypercharge and A' field strength tensors [2–7]. This mixing provides a potential portal through which dark photons may be produced if kinematically allowed. If the kinetic mixing arises due to processes whose amplitudes involve one or two loops containing high-mass particles, perhaps even at the Planck scale, then $10^{-12} \lesssim \epsilon^2 \lesssim 10^{-4}$ is expected [1]. Fully exploring this *few-loop* range of kinetic-mixing strength is an important goal of dark-sector physics.

Constraints have been placed on visible A' decays by previous beam-dump [7–21], fixed-target [22–24], collider [25–28], and rare-meson-decay [29–38] experiments. The few-loop region is ruled out for dark photon masses $m(A') \lesssim 10 \text{ MeV}$ ($c = 1$ throughout this Letter). Additionally, the region $\epsilon^2 \gtrsim 5 \times 10^{-7}$ is excluded for $m(A') < 10.2 \text{ GeV}$, along with about half of the remaining few-loop region below the dimuon threshold. Many ideas have been proposed to further explore the $[m(A'), \epsilon^2]$

parameter space [39–51], including an inclusive search for $A' \rightarrow \mu^+\mu^-$ decays with the LHCb experiment, which is predicted to provide sensitivity to large regions of otherwise inaccessible parameter space using data to be collected during Run 3 of the LHC (2021–2023) [52].

A dark photon produced in proton-proton, pp , collisions via γ - A' mixing inherits the production mechanisms of an off-shell photon with $m(\gamma^*) = m(A')$; therefore, both the production and decay kinematics of the $A' \rightarrow \mu^+\mu^-$ and $\gamma^* \rightarrow \mu^+\mu^-$ processes are identical. Furthermore, the expected $A' \rightarrow \mu^+\mu^-$ signal yield is given by [52]

$$n_{\text{ex}}^{A'}[m(A'), \epsilon^2] = \epsilon^2 \left(\frac{n_{\text{ob}}^{\gamma^*}[m(A')]}{2\Delta m} \right) \mathcal{F}[m(A')] \epsilon_{\gamma^*}^{A'}[m(A'), \tau(A')], \quad (1)$$

where $n_{\text{ob}}^{\gamma^*}[m(A')]$ is the observed prompt $\gamma^* \rightarrow \mu^+\mu^-$ yield in a small $\pm\Delta m$ window around $m(A')$, the function $\mathcal{F}[m(A')]$ includes phase-space and other known factors, and $\epsilon_{\gamma^*}^{A'}[m(A'), \tau(A')]$ is the ratio of the $A' \rightarrow \mu^+\mu^-$ and $\gamma^* \rightarrow \mu^+\mu^-$ detection efficiencies, which depends on the A' lifetime, $\tau(A')$. If A' decays to invisible final states are negligible, then $\tau(A') \propto [m(A')\epsilon^2]^{-1}$ and $A' \rightarrow \mu^+\mu^-$ decays can potentially be reconstructed as displaced from the primary pp vertex (PV) when the product $m(A')\epsilon^2$ is small. When $\tau(A')$ is small compared to the experimental resolution, $A' \rightarrow \mu^+\mu^-$ decays are reconstructed as promptlike and are experimentally indistinguishable from prompt $\gamma^* \rightarrow \mu^+\mu^-$ production, resulting in $\epsilon_{\gamma^*}^{A'}[m(A'), \tau(A')] \approx 1$. This facilitates a fully data-driven search and the cancellation of most experimental systematic effects, since the observed $A' \rightarrow \mu^+\mu^-$ yields, $n_{\text{ob}}^{A'}[m(A')]$, can be normalized to $n_{\text{ex}}^{A'}[m(A'), \epsilon^2]$ to obtain constraints on ϵ^2 .

*Full author list given at the end of the article.

Published by the American Physical Society under the terms of the Creative Commons Attribution 4.0 International license. Further distribution of this work must maintain attribution to the author(s) and the published article's title, journal citation, and DOI. Funded by SCOAP³.

This Letter presents searches for both promptlike and long-lived dark photons produced in pp collisions at a center-of-mass energy of 13 TeV, using $A' \rightarrow \mu^+\mu^-$ decays and a data sample corresponding to an integrated luminosity of 1.6 fb^{-1} collected with the LHCb detector in 2016. The promptlike A' search is performed from near the dimuon threshold up to 70 GeV, above which the $m(\mu^+\mu^-)$ spectrum is dominated by the Z boson. The long-lived A' search is restricted to the mass range $214 < m(A') < 350 \text{ MeV}$, where the data sample potentially provides sensitivity.

The LHCb detector is a single-arm forward spectrometer covering the pseudorapidity range $2 < \eta < 5$, described in detail in Refs. [53,54]. Simulated data samples, which are used to validate the analysis, are produced using the software described in Refs. [55–57]. The online event selection is performed by a trigger [58], which consists of a hardware stage using information from the calorimeter and muon systems, followed by a software stage, which performs a full event reconstruction. At the hardware stage, events are required to have a muon with $p_T \gtrsim 1.8 \text{ GeV}$, where p_T is the momentum transverse to the beam direction, or a dimuon in which the product of the p_T of each muon is in excess of $(\approx 1.5 \text{ GeV})^2$. The long-lived A' search also uses events selected at the hardware stage independently of the $A' \rightarrow \mu^+\mu^-$ candidate. In the software stage, $A' \rightarrow \mu^+\mu^-$ candidates are built from two oppositely charged tracks that form a good quality vertex and satisfy stringent muon-identification criteria. The muons are required to have $2 < \eta < 4.5$, $p_T > 0.5$ (1.0) GeV, momentum $p > 10$ (20) GeV, and be inconsistent (consistent) with originating from the PV in the long-lived (promptlike) A' search. Finally, the A' candidates are required to satisfy $p_T > 1 \text{ GeV}$, $2 < \eta < 4.5$, and have a decay topology consistent with originating from the PV.

The promptlike A' search is based on a data sample where all online-reconstructed particles are stored, but most lower-level information is discarded, greatly reducing the event size. This data-storage strategy, made possible by advances in the LHCb data-taking scheme introduced in 2015 [59,60], permits the recording of all events that contain a promptlike dimuon candidate without placing any requirements on $m(\mu^+\mu^-)$. The $m(\mu^+\mu^-)$ spectrum recorded by the trigger is provided in the Supplemental Material [61].

Three main types of background contribute to the promptlike A' search: prompt $\gamma^* \rightarrow \mu^+\mu^-$ production, which is irreducible; resonant decays to $\mu^+\mu^-$, whose mass-peak regions are avoided in the search; and various types of misreconstruction. The misreconstruction background consists of three dominant contributions: double misidentification of prompt hadrons as muons, hh ; a misidentified prompt hadron combined with a muon produced in a decay of a hadron containing a heavy-flavor quark, Q , where the muon is misreconstructed as

promptlike, $h\mu_Q$; and the misreconstruction of two muons produced in Q -hadron decays, $\mu_Q\mu_Q$. These backgrounds are highly suppressed by the stringent muon-identification and promptlike requirements applied in the trigger; however, in the region $[m(\phi), m(\Upsilon)]$, the misreconstructed backgrounds overwhelm the signal-like $\gamma^* \rightarrow \mu^+\mu^-$ contribution.

For masses below (above) the ϕ meson mass, dark photons are expected to be predominantly produced in meson-decay (Drell-Yan) processes in pp collisions at LHCb. A well-known signature of Drell-Yan production is dimuons that are largely isolated, and a high-mass dark photon would inherit this property. The signal sensitivity is enhanced by applying a jet-based isolation requirement for $m(A') > m(\phi)$, which improves the sensitivity by up to a factor of 2 at low masses and by $\mathcal{O}(10\%)$ for $m(A') > 10 \text{ GeV}$. Jet reconstruction is performed by clustering charged and neutral particle-flow candidates [62] using the anti- k_T clustering algorithm [63] with $R = 0.5$ as implemented in FASTJET [64]. Muons with $p_T(\mu)/p_T(\text{jet}) < 0.7$ are rejected, where the contribution to $p_T(\text{jet})$ from the other muon is excluded if both muons are clustered in the same jet, as this is found to provide nearly optimal sensitivity for all $m(A') > m(\phi)$. Figure 1 shows the resulting promptlike $m(\mu^+\mu^-)$ spectrum using Δm bins that are $\sigma[m(\mu^+\mu^-)]/2$ wide, where $\sigma[m(\mu^+\mu^-)]$ is the mass resolution which varies from about 0.7 MeV near threshold to 0.7 GeV at $m(\mu^+\mu^-) = 70 \text{ GeV}$.

The promptlike A' search strategy involves determining the observed $A' \rightarrow \mu^+\mu^-$ yields from fits to the $m(\mu^+\mu^-)$ spectrum, and normalizing them using Eq. (1) to obtain constraints on ε^2 . To determine $n_{\text{ob}}^{\gamma^*}[m(A')]$ for use in Eq. (1), binned extended maximum likelihood fits are performed using the dimuon vertex-fit quality, $\chi_{\text{VF}}^2(\mu^+\mu^-)$, and $\min[\chi_{\text{IP}}^2(\mu^\pm)]$ distributions, where $\chi_{\text{IP}}^2(\mu)$ is defined as the difference in $\chi_{\text{VF}}^2(\text{PV})$ when the PV is reconstructed with and without the muon track. The $\chi_{\text{VF}}^2(\mu^+\mu^-)$ and $\min[\chi_{\text{IP}}^2(\mu^\pm)]$ fits are performed independently at each mass, with the mean of the $n_{\text{ob}}^{\gamma^*}[m(A')]$ results used as the nominal value and half the difference assigned as a systematic uncertainty.

Both fit quantities are built from features that approximately follow χ^2 probability density functions (PDFs) with

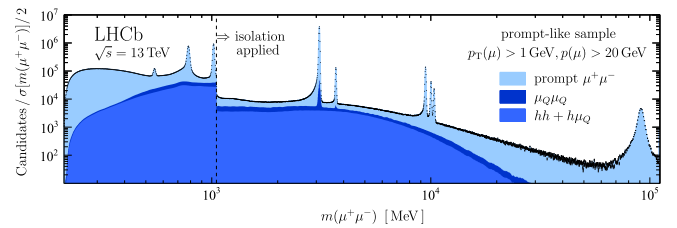


FIG. 1. Promptlike mass spectrum, where the categorization of the data as prompt $\mu^+\mu^-$, $\mu_Q\mu_Q$, and $hh + h\mu_Q$ is determined using the fits described in the text.

minimal mass dependence. The prompt-dimuon PDFs are taken directly from data at $m(J/\psi)$ and $m(Z)$, where prompt resonances are dominant (see Fig. 1). Small p_T -dependent corrections are applied to obtain the PDFs at all other masses. These PDFs are validated near threshold, at $m(\phi)$, and at $m(\Upsilon(1S))$, where the data predominantly consist of prompt dimuons. The sum of the hh and $h\mu_Q$ contributions, which each involve misidentified prompt hadrons, is determined using same-sign $\mu^\pm\mu^\pm$ candidates that satisfy all of the promptlike criteria. A correction is applied to the observed $\mu^\pm\mu^\pm$ yield at each mass to account for the difference in the production rates of $\pi^+\pi^-$ and $\pi^\pm\pi^\pm$, since double misidentified $\pi^+\pi^-$ pairs are the dominant source of the hh background. This correction, which is derived using a promptlike dipion data sample weighted by p_T -dependent muon-misidentification probabilities, is as large as a factor of 2 near $m(\rho)$ but negligible for $m(\mu^+\mu^-) \gtrsim 2$ GeV. The PDFs for the $\mu_Q\mu_Q$ background, which involves muon pairs produced in Q -hadron decays that occur displaced from the PV, are obtained from simulation. These muons are rarely produced at the same spatial point unless the decay chain involves charmonium. Example $\min[\chi^2_{\text{IP}}(\mu^\pm)]$ fit results are provided in Ref. [61], while Fig. 1 shows the resulting data categorizations. Finally, the $n_{\text{obs}}^A[m(A')]$ yields are corrected for bin migration due to bremsstrahlung, and the small expected Bethe-Heitler contribution is subtracted [52].

The promptlike mass spectrum is scanned in steps of $\sigma[m(\mu^+\mu^-)]/2$ searching for $A' \rightarrow \mu^+\mu^-$ contributions. At each mass, a binned extended maximum likelihood fit is performed using all promptlike candidates in a $\pm 12.5\sigma[m(\mu^+\mu^-)]$ window around $m(A')$. The profile likelihood is used to determine the p value and the confidence interval for $n_{\text{obs}}^A[m(A')]$, from which an upper limit at 90% confidence level (C.L.) is obtained. The signal PDFs are determined using a combination of simulated $A' \rightarrow \mu^+\mu^-$ decays and the widths of the large resonance peaks observed in the data. The strategy proposed in Ref. [65] is used to select the background model and assign its uncertainty. This method takes as input a large set of potential background components, which here includes all Legendre modes up to tenth order and dedicated terms for known resonances, and then performs a data-driven model-selection process whose uncertainty is included in the profile likelihood following Ref. [66]. More details about the fits, including discussion on peaking backgrounds, are provided in Ref. [61]. The most significant excess is 3.3σ at $m(A') \approx 5.8$ GeV, corresponding to a p value of 38% after accounting for the trials factor due to the number of promptlike signal hypotheses.

Regions of the $[m(A'), \epsilon^2]$ parameter space where the upper limit on $n_{\text{obs}}^A[m(A')]$ is less than $n_{\text{ex}}^A[m(A'), \epsilon^2]$ are excluded at 90% C.L. Figure 2 shows that the constraints placed on promptlike dark photons are comparable to the

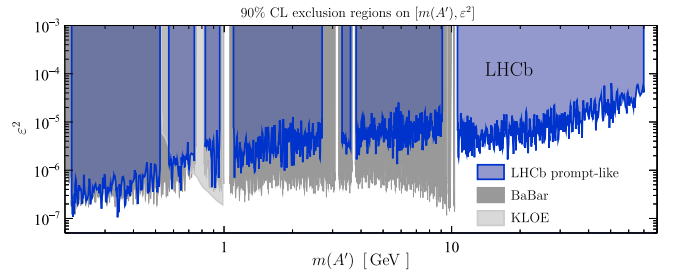


FIG. 2. Regions of the $[m(A'), \epsilon^2]$ parameter space excluded at 90% C.L. by the promptlike A' search compared to the best existing limits [27,38].

best existing limits below 0.5 GeV, and are the most stringent for $10.6 < m(A') < 70$ GeV. In the latter mass range, a non-negligible model-dependent mixing with the Z boson introduces additional kinetic-mixing parameters altering Eq. (1); however, the expanded A' model space is highly constrained by precision electroweak measurements. This search adopts the parameter values suggested in Refs. [67,68]. The LHCb detector response is found to be independent of which quark-annihilation process produces the dark photon above 10 GeV, making it easy to recast the results in Fig. 2 for other models.

For the long-lived dark photon search, the stringent criteria applied in the trigger make contamination from prompt muon candidates negligible. The dominant background contributions to the long-lived A' search are as follows: photon conversions to $\mu^+\mu^-$ in the silicon-strip vertex detector (the VELO) that surrounds the pp interaction region [69]; b -hadron decays where two muons are produced in the decay chain; and the low-mass tail from $K_S^0 \rightarrow \pi^+\pi^-$ decays, where both pions are misidentified as muons. Additional sources of background are negligible, e.g., kaon and hyperon decays, and Q -hadron decays producing a muon and a hadron that is misidentified as a muon.

Photon conversions in the VELO dominate the long-lived data sample at low masses. A new method was recently developed for identifying particles created in secondary interactions with the VELO material. A high-precision three-dimensional material map was produced from a data sample of secondary hadronic interactions. Using this material map, along with properties of the $A' \rightarrow \mu^+\mu^-$ decay vertex and muon tracks, a p value is assigned to the photon-conversion hypothesis for each long-lived $A' \rightarrow \mu^+\mu^-$ candidate. A mass-dependent requirement is applied to these p values that reduces the expected photon-conversion yields to a negligible level.

A characteristic signature of muons produced in b -hadron decays is the presence of additional displaced tracks. Events are rejected if they are selected by the inclusive Q -hadron software trigger [70] independently of the presence of the $A' \rightarrow \mu^+\mu^-$ candidate. Furthermore, two boosted decision tree (BDT) classifiers, originally

developed for studying $B_{(s)}^0 \rightarrow \mu^+\mu^-$ decays [71], are used to identify other tracks in the event that are consistent with having originated from the same b -hadron decay as the signal muon candidates. The requirements placed on the BDT responses, which are optimized using a data sample of K_S^0 decays as a signal proxy, reject 70% of the b -hadron background at a cost of about 10% loss in signal efficiency.

As in the promptlike A' search, the normalization is based on Eq. (1); however, in the long-lived A' search, $\epsilon_{\gamma^*}^{A'}[m(A'), \tau(A')]$ is not unity, in part because the efficiency depends on the decay time, t . Furthermore, the looser kinematic, muon-identification, and hardware-trigger requirements applied to long-lived $A' \rightarrow \mu^+\mu^-$ candidates, cf. promptlike candidates, increase the efficiency by a factor of 7 to 10, ignoring t -dependent effects. These $m(A')$ -dependent factors are determined using a small control data sample of dimuon candidates consistent with originating from the PV, but otherwise satisfying the long-lived criteria. A relative 10% systematic uncertainty is assigned to the long-lived $A' \rightarrow \mu^+\mu^-$ normalization due to background contamination in the control sample.

The fact that the kinematics are identical for $A' \rightarrow \mu^+\mu^-$ and prompt $\gamma^* \rightarrow \mu^+\mu^-$ decays for $m(A') = m(\gamma^*)$ enables the t dependence of the signal efficiency to be determined using a data-driven approach. For each value of $[m(A'), \tau(A')]$, prompt $\gamma^* \rightarrow \mu^+\mu^-$ candidates in the control data sample near $m(A')$ are resampled many times as long-lived $A' \rightarrow \mu^+\mu^-$ decays, and all t -dependent properties, e.g., $\min[\chi_{\text{IP}}^2(\mu^\pm)]$, are recalculated based on the resampled decay-vertex locations. This approach is validated in simulation by using prompt $A' \rightarrow \mu^+\mu^-$ decays to predict the properties of long-lived $A' \rightarrow \mu^+\mu^-$ decays, and based on these studies a 2% systematic uncertainty is assigned to the signal efficiencies. The $\epsilon_{\gamma^*}^{A'}[m(A'), \tau(A')]$ values integrated over t are provided in Ref. [61].

A scan is again performed in discrete steps of $\sigma[m(\mu^+\mu^-)]/2$ looking for $A' \rightarrow \mu^+\mu^-$ contributions; however, in this case, discrete steps in $\tau(A')$ are also considered. Binned extended maximum likelihood fits are performed using all long-lived candidates and the three-dimensional feature space of $m(\mu^+\mu^-)$, t , and the consistency of the decay topology as quantified in the decay-fit χ_{DF}^2 , which has three degrees of freedom (the data distribution is provided in Ref. [61]). The expected conversion contribution is derived in each bin from the number of candidates rejected by the conversion criterion. Two large control data samples are used to develop and validate the modeling of the b -hadron and K_S^0 contributions: candidates that fail the b -hadron suppression requirements, and candidates that fail but nearly satisfy the muon-identification requirements. The profile likelihood is used to obtain the p values and confidence intervals on $n_{\text{ob}}^{A'}[m(A'), \tau(A')]$. The most significant excess occurs at $m(A') = 239$ MeV and $\tau(A') = 0.86$ ps, where the p value corresponds to 3.0σ .

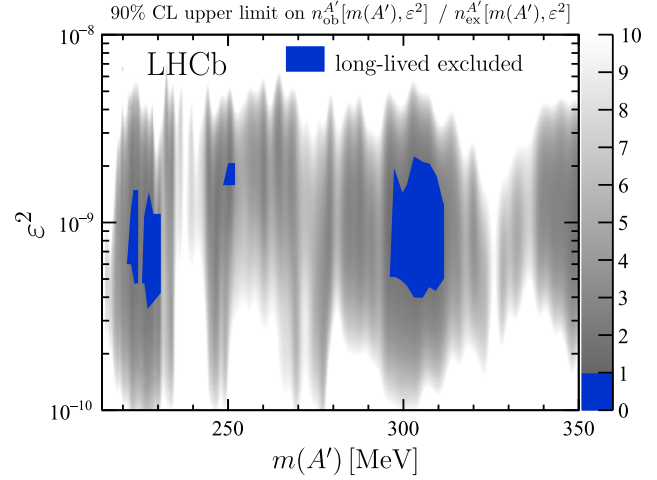


FIG. 3. Ratio of the observed upper limit on $n_{\text{ob}}^{A'}[m(A'), \epsilon^2]$ at 90% C.L. to its expected value, where regions less than unity are excluded. There are no constraints from previous experiments in this region.

Considering only the long-lived-search trials factor reduces this to 2.0σ . More details about these fits are provided in Ref. [61].

Under the assumption that A' decays to invisible final states are negligible, there is a fixed (and known) relationship between $\tau(A')$ and ϵ^2 at each mass [52]; therefore, the upper limits on $n_{\text{ob}}^{A'}[m(A'), \tau(A')]$ can be translated into limits on $n_{\text{ob}}^{A'}[m(A'), \epsilon^2]$. Regions of the $[m(A'), \epsilon^2]$ parameter space where the upper limit on $n_{\text{ob}}^{A'}[m(A'), \epsilon^2]$ is less than $n_{\text{ex}}^{A'}[m(A'), \epsilon^2]$ are excluded at 90% C.L. (see Fig. 3). While only small regions of $[m(A'), \epsilon^2]$ space are excluded, a sizable portion of this parameter space will soon become accessible as more data are collected.

In summary, searches are performed for both promptlike and long-lived dark photons produced in pp collisions at a center-of-mass energy of 13 TeV, using $A' \rightarrow \mu^+\mu^-$ decays and a data sample corresponding to an integrated luminosity of 1.6 fb^{-1} collected with the LHCb detector during 2016. The promptlike A' search covers the mass range from near the dimuon threshold up to 70 GeV, while the long-lived A' search is restricted to the low-mass region $214 < m(A') < 350$ MeV. No evidence for a signal is found, and 90% C.L. exclusion regions are set on the γ - A' kinetic-mixing strength. The constraints placed on promptlike dark photons are the most stringent to date for the mass range $10.6 < m(A') < 70$ GeV, and are comparable to the best existing limits for $m(A') < 0.5$ GeV. The search for long-lived dark photons is the first to achieve sensitivity using a displaced-vertex signature.

These results demonstrate the unique sensitivity of the LHCb experiment to dark photons, even using a data sample collected with a trigger that is inefficient for low-mass $A' \rightarrow \mu^+\mu^-$ decays. Using knowledge gained from this analysis, the software-trigger efficiency for

low-mass dark photons has been significantly improved for 2017 data taking. Looking forward to Run 3, the planned increase in luminosity and removal of the hardware-trigger stage should increase the number of expected $A' \rightarrow \mu^+\mu^-$ decays in the low-mass region by a factor of $\mathcal{O}(100\text{--}1000)$ compared to the 2016 data sample.

We express our gratitude to our colleagues in the CERN accelerator departments for the excellent performance of the LHC. We thank the technical and administrative staff at the LHCb institutes. We acknowledge support from CERN and from the national agencies: CAPES, CNPq, FAPERJ and FINEP (Brazil); MOST and NSFC (China); CNRS/IN2P3 (France); BMBF, DFG and MPG (Germany); INFN (Italy); NWO (The Netherlands); MNiSW and NCN (Poland); MEN/IFA (Romania); MinES and FASO (Russia); MinECo (Spain); SNSF and SER (Switzerland); NASU (Ukraine); STFC (United Kingdom); NSF (USA). We acknowledge the computing resources that are provided by CERN, IN2P3 (France), KIT and DESY (Germany), INFN (Italy), SURF (Netherlands), PIC (Spain), GridPP (United Kingdom), RRCKI and Yandex LLC (Russia), CSCS (Switzerland), IFIN-HH (Romania), CBPF (Brazil), PL-GRID (Poland) and OSC (USA). We are indebted to the communities behind the multiple open-source software packages on which we depend. Individual groups or members have received support from AvH Foundation (Germany), EPLANET, Marie Skłodowska-Curie Actions and ERC (European Union), ANR, Labex P2IO, ENIGMASS and OCEVU, and Région Auvergne-Rhône-Alpes (France), RFBR and Yandex LLC (Russia), GVA, XuntaGal and GENCAT (Spain), Herchel Smith Fund, the Royal Society, the English-Speaking Union and the Leverhulme Trust (United Kingdom).

[1] J. Alexander *et al.*, Dark Sectors 2016 Workshop: Community Report, [arXiv:1608.08632](https://arxiv.org/abs/1608.08632).
 [2] L. B. Okun, Limits of electrodynamicis: Paraphotons?, *Zh. Eksp. Teor. Fiz.* **83**, 892 (1982) [*Sov. Phys. JETP* **56**, 502 (1982)].
 [3] P. Galison and A. Manohar, Two Z 's or not two Z 's?, *Phys. Lett.* **136B**, 279 (1984).
 [4] B. Holdom, Two $U(1)$'s and ϵ charge shifts, *Phys. Lett.* **166B**, 196 (1986).
 [5] M. Pospelov, A. Ritz, and M. B. Voloshin, Secluded WIMP dark matter, *Phys. Lett. B* **662**, 53 (2008).
 [6] N. Arkani-Hamed, D. P. Finkbeiner, T. R. Slatyer, and N. Weiner, A theory of dark matter, *Phys. Rev. D* **79**, 015014 (2009).
 [7] J. D. Bjorken, R. Essig, P. Schuster, and N. Toro, New fixed-target experiments to search for dark gauge forces, *Phys. Rev. D* **80**, 075018 (2009).

[8] F. Bergsma *et al.* (CHARM Collaboration), A search for decays of heavy neutrinos in the mass range 0.5 GeV to 2.8 GeV, *Phys. Lett.* **166B**, 473 (1986).
 [9] A. Konaka *et al.*, Search for Neutral Particles in Electron-Beam-Dump Experiment, *Phys. Rev. Lett.* **57**, 659 (1986).
 [10] E. M. Riordan *et al.*, Search for Short-Lived Axions in an Electron-Beam-Dump Experiment, *Phys. Rev. Lett.* **59**, 755 (1987).
 [11] J. D. Bjorken, S. Ecklund, W. R. Nelson, A. Abashian, C. Church, B. Lu, L. W. Mo, T. A. Nunamaker, and P. Rassmann, Search for neutral metastable penetrating particles produced in the SLAC beam dump, *Phys. Rev. D* **38**, 3375 (1988).
 [12] A. Bross, M. Crisler, S. H. Pordes, J. Volk, S. Errede, and J. Wrbanek, A Search for Short-Lived Particles Produced in an Electron Beam Dump, *Phys. Rev. Lett.* **67**, 2942 (1991).
 [13] M. Davier and H. Nguyen Ngoc, An unambiguous search for a light Higgs boson, *Phys. Lett. B* **229**, 150 (1989).
 [14] C. Athanassopoulos *et al.* (LSND Collaboration), Evidence for $\nu_\mu \rightarrow \nu_e$ oscillations from pion decay in flight neutrinos, *Phys. Rev. C* **58**, 2489 (1998).
 [15] P. Astier *et al.* (NOMAD Collaboration), Search for heavy neutrinos mixing with tau neutrinos, *Phys. Lett. B* **506**, 27 (2001).
 [16] S. Adler *et al.* (E787 Collaboration), Further search for the decay $K^+ \rightarrow \pi^+\nu\bar{\nu}$ in the momentum region $p < 195$ MeV/c, *Phys. Rev. D* **70**, 037102 (2004).
 [17] A. V. Artamonov *et al.* (BNL-E949 Collaboration), Study of the decay $K^+ \rightarrow \pi^+\nu\bar{\nu}$ in the momentum region $140 < P_\pi < 199$ MeV/c, *Phys. Rev. D* **79**, 092004 (2009).
 [18] R. Essig, R. Harnik, J. Kaplan, and N. Toro, Discovering new light states at neutrino experiments, *Phys. Rev. D* **82**, 113008 (2010).
 [19] J. Blümlein and J. Brunner, New exclusion limits for dark gauge forces from beam-dump data, *Phys. Lett. B* **701**, 155 (2011).
 [20] S. N. Gninenko, Constraints on sub-GeV hidden sector gauge bosons from a search for heavy neutrino decays, *Phys. Lett. B* **713**, 244 (2012).
 [21] J. Blümlein and J. Brunner, New exclusion limits on dark gauge forces from proton bremsstrahlung in beam-dump data, *Phys. Lett. B* **731**, 320 (2014).
 [22] S. Abrahamyan *et al.* (APEX Collaboration), Search for a New Gauge Boson in Electron-Nucleus Fixed-Target Scattering by the APEX Experiment, *Phys. Rev. Lett.* **107**, 191804 (2011).
 [23] H. Merkel *et al.* (A1 Collaboration), Search at the Mainz Microtron for Light Massive Gauge Bosons Relevant for the Muon $g-2$ Anomaly, *Phys. Rev. Lett.* **112**, 221802 (2014).
 [24] H. Merkel *et al.* (A1 Collaboration), Search for Light Gauge Bosons of the Dark Sector at the Mainz Microtron, *Phys. Rev. Lett.* **106**, 251802 (2011).
 [25] B. Aubert *et al.* (BABAR Collaboration), Search for Dimuon Decays of a Light Scalar Boson in Radiative Transitions $\Upsilon \rightarrow \gamma A^0$, *Phys. Rev. Lett.* **103**, 081803 (2009).
 [26] D. Curtin *et al.*, Exotic decays of the 125 GeV Higgs boson, *Phys. Rev. D* **90**, 075004 (2014).
 [27] J. P. Lees *et al.* (BABAR Collaboration), Search for a Dark Photon in e^+e^- Collisions at BABAR, *Phys. Rev. Lett.* **113**, 201801 (2014).

- [28] M. Ablikim *et al.* (BESIII Collaboration), Dark photon search in the mass range between 1.5 and 3.4 GeV/c², *Phys. Lett. B* **774**, 252 (2017).
- [29] G. Bernardi *et al.*, Search for neutrino decay, *Phys. Lett.* **166B**, 479 (1986).
- [30] R. Meijer Drees *et al.* (SINDRUM I Collaboration), Search for Weakly Interacting Neutral Bosons Produced in π^-p Interactions at Rest and Decaying into e^+e^- Pairs, *Phys. Rev. Lett.* **68**, 3845 (1992).
- [31] F. Archilli *et al.* (KLOE-2 Collaboration), Search for a vector gauge boson in ϕ meson decays with the KLOE detector, *Phys. Lett. B* **706**, 251 (2012).
- [32] S. N. Gninenko, Stringent limits on the $\pi^0 \rightarrow \gamma X$, $X \rightarrow e^+e^-$ decay from neutrino experiments and constraints on new light gauge bosons, *Phys. Rev. D* **85**, 055027 (2012).
- [33] D. Babusci *et al.* (KLOE-2 Collaboration), Limit on the production of a light vector gauge boson in ϕ meson decays with the KLOE detector, *Phys. Lett. B* **720**, 111 (2013).
- [34] P. Adlarson *et al.* (WASA-at-COSY Collaboration), Search for a dark photon in the $\pi^0 \rightarrow e^+e^-\gamma$ decay, *Phys. Lett. B* **726**, 187 (2013).
- [35] G. Agakishiev *et al.* (HADES Collaboration), Searching a dark photon with HADES, *Phys. Lett. B* **731**, 265 (2014).
- [36] A. Adare *et al.* (PHENIX Collaboration), Search for dark photons from neutral meson decays in pp and dAu collisions at $\sqrt{s_{NN}} = 200$ GeV, *Phys. Rev. C* **91**, 031901 (2015).
- [37] J. R. Batley *et al.* (NA48/2 Collaboration), Search for the dark photon in π^0 decays, *Phys. Lett. B* **746**, 178 (2015).
- [38] A. Anastasi *et al.* (KLOE-2 Collaboration), Limit on the production of a new vector boson in $e^+e^- \rightarrow U\gamma$, $U \rightarrow \pi^+\pi^-$ with the KLOE experiment, *Phys. Lett. B* **757**, 356 (2016).
- [39] R. Essig, P. Schuster, N. Toro, and B. Wojtsekhowski, An electron fixed target experiment to search for a new vector boson a' decaying to e^+e^- , *J. High Energy Phys.* **02** (2011) 009.
- [40] M. Freytsis, G. Ovanesyan, and J. Thaler, Dark force detection in low energy ep collisions, *J. High Energy Phys.* **01** (2010) 111.
- [41] J. Balewski *et al.*, DarkLight: A search for dark forces at the Jefferson Laboratory free-electron laser facility, [arXiv:1307.4432](https://arxiv.org/abs/1307.4432).
- [42] B. Wojtsekhowski, D. Nikolenko, and I. Rachek, Searching for a new force at VEPP-3, [arXiv:1207.5089](https://arxiv.org/abs/1207.5089).
- [43] T. Beranek, H. Merkel, and M. Vanderhaeghen, Theoretical framework to analyze searches for hidden light gauge bosons in electron scattering fixed target experiments, *Phys. Rev. D* **88**, 015032 (2013).
- [44] B. Echenard, R. Essig, and Y.-M. Zhong, Projections for dark photon searches at Mu3e, *J. High Energy Phys.* **01** (2015) 113.
- [45] M. Battaglieri *et al.*, The heavy photon search test detector, *Nucl. Instrum. Methods Phys. Res., Sect. A* **777**, 91 (2015).
- [46] S. Alekhin *et al.*, A facility to search for hidden particles at the CERN SPS: The SHiP physics case, *Rep. Prog. Phys.* **79**, 124201 (2016).
- [47] S. Gardner, R. J. Holt, and A. S. Tadepalli, New prospects in fixed target searches for dark forces with the SeaQuest experiment at Fermilab, *Phys. Rev. D* **93**, 115015 (2016).
- [48] P. Ilten, J. Thaler, M. Williams, and W. Xue, Dark photons from charm mesons at LHCb, *Phys. Rev. D* **92**, 115017 (2015).
- [49] D. Curtin, R. Essig, S. Gori, and J. Shelton, Illuminating dark photons with high-energy colliders, *J. High Energy Phys.* **02** (2015) 157.
- [50] M. He, X.-G. He, and C.-K. Huang, Dark photon search at a circular e^+e^- collider, *Int. J. Mod. Phys. A* **32**, 1750138 (2017).
- [51] J. Kozaczuk, Dark photons from nuclear transitions, [arXiv:1708.06349](https://arxiv.org/abs/1708.06349) [*Phys. Rev. D* (to be published)].
- [52] P. Ilten, Y. Soreq, J. Thaler, M. Williams, and W. Xue, Proposed Inclusive Dark Photon Search at LHCb, *Phys. Rev. Lett.* **116**, 251803 (2016).
- [53] A. A. Alves Jr. *et al.* (LHCb Collaboration), The LHCb detector at the LHC, *J. Instrum.* **3**, S08005 (2008).
- [54] R. Aaij *et al.* (LHCb Collaboration), LHCb detector performance, *Int. J. Mod. Phys. A* **30**, 1530022 (2015).
- [55] T. Sjöstrand, S. Ask, J. R. Christiansen, R. Corke, N. Desai, P. Ilten, S. Mrenna, S. Prestel, C. O. Rasmussen, and P. Z. Skands, An introduction to PYTHIA 8.2, *Comput. Phys. Commun.* **191**, 159 (2015); T. Sjöstrand, S. Mrenna, and P. Skands, A brief introduction to PYTHIA 8.1, *Comput. Phys. Commun.* **178**, 852 (2008).
- [56] I. Belyaev *et al.*, Handling of the generation of primary events in Gauss, the LHCb simulation framework, *J. Phys. Conf. Ser.* **331**, 032047 (2011).
- [57] J. Allison *et al.* (Geant4 Collaboration), Geant4 developments and applications, *IEEE Trans. Nucl. Sci.* **53**, 270 (2006); S. Agostinelli *et al.* (Geant4 Collaboration), Geant4: A simulation toolkit, *Nucl. Instrum. Methods Phys. Res., Sect. A* **506**, 250 (2003).
- [58] R. Aaij *et al.*, The LHCb trigger and its performance in 2011, *J. Instrum.* **8**, P04022 (2013).
- [59] G. Dujany and B. Storaci, Real-time alignment and calibration of the LHCb Detector in Run II, *J. Phys. Conf. Ser.* **664**, 082010 (2015).
- [60] R. Aaij *et al.*, Tesla: An application for real-time data analysis in high energy physics, *Comput. Phys. Commun.* **208**, 35 (2016).
- [61] See Supplemental Material at <http://link.aps.org/supplemental/10.1103/PhysRevLett.120.061801> for additional fit details and figures.
- [62] R. Aaij *et al.* (LHCb Collaboration), Study of forward $Z + \text{jet}$ production in pp collisions at $\sqrt{s} = 7$ TeV, *J. High Energy Phys.* **01** (2014) 033.
- [63] M. Cacciari, G. P. Salam, and G. Soyez, The anti- k_T jet clustering algorithm, *J. High Energy Phys.* **04** (2008) 063.
- [64] M. Cacciari, G. P. Salam, and G. Soyez, FASTJET user manual, *Eur. Phys. J. C* **72**, 1896 (2012).
- [65] M. Williams, A novel approach to the bias-variance problem in bump hunting, *J. Instrum.* **12**, P09034 (2017).
- [66] P. D. Dauncey, M. Kenzie, N. Wardle, and G. J. Davies, Handling uncertainties in background shapes, *J. Instrum.* **10**, P04015 (2015).
- [67] S. Cassel, D. M. Ghilencea, and G. G. Ross, Electroweak and dark matter constraints on a Z' in models with a hidden valley, *Nucl. Phys.* **B827**, 256 (2010).
- [68] J. M. Cline, G. Dupuis, Z. Liu, and W. Xue, The windows for kinetically mixed Z' -mediated dark matter and the

- galactic center gamma ray excess, *J. High Energy Phys.* **08** (2014) 131.
- [69] R. Aaij *et al.*, Performance of the LHCb vertex locator, *J. Instrum.* **9**, P09007 (2014).
- [70] T. Likhomanenko, P. Iiten, E. Khairullin, A. Rogozhnikov, A. Ustyuzhanin, and M. Williams, LHCb topological trigger reoptimization, *J. Phys. Conf. Ser.* **664**, 082025 (2015).
- [71] R. Aaij *et al.* (LHCb Collaboration), Measurement of the $B_s^0 \rightarrow \mu^+\mu^-$ Branching Fraction and Effective Lifetime and Search for $B^0 \rightarrow \mu^+\mu^-$ Decays, *Phys. Rev. Lett.* **118**, 191801 (2017).

R. Aaij,⁴⁰ B. Adeva,³⁹ M. Adinolfi,⁴⁸ Z. Ajaltouni,⁵ S. Akar,⁵⁹ J. Albrecht,¹⁰ F. Alessio,⁴⁰ M. Alexander,⁵³ A. Alfonso Alberio,³⁸ S. Ali,⁴³ G. Alkhazov,³¹ P. Alvarez Cartelle,⁵⁵ A. A. Alves Jr.,⁵⁹ S. Amato,² S. Amerio,²³ Y. Amhis,⁷ L. An,³ L. Anderlini,¹⁸ G. Andreassi,⁴¹ M. Andreotti,^{17,a} J. E. Andrews,⁶⁰ R. B. Appleby,⁵⁶ F. Archilli,⁴³ P. d'Argent,¹² J. Arnau Romeu,⁶ A. Artamonov,³⁷ M. Artuso,⁶¹ E. Aslanides,⁶ M. Atzeni,⁴² G. Auremma,²⁶ M. Baalouch,⁵ I. Babuschkin,⁵⁶ S. Bachmann,¹² J. J. Back,⁵⁰ A. Badalov,^{38,b} C. Baesso,⁶² S. Baker,⁵⁵ V. Balagura,^{7,c} W. Baldini,¹⁷ A. Baranov,³⁵ R. J. Barlow,⁵⁶ C. Barschel,⁴⁰ S. Barsuk,⁷ W. Barter,⁵⁶ F. Baryshnikov,³² V. Batozskaya,²⁹ V. Battista,⁴¹ A. Bay,⁴¹ L. Beaucourt,⁴ J. Beddow,⁵³ F. Bedeschi,²⁴ I. Bediaga,¹ A. Beiter,⁶¹ L. J. Bel,⁴³ N. Belyi,⁶³ V. Bellee,⁴¹ N. Belloli,^{21,d} K. Belous,³⁷ I. Belyaev,^{32,40} E. Ben-Haim,⁸ G. Bencivenni,¹⁹ S. Benson,⁴³ S. Beranek,⁹ A. Berezhniov,³³ R. Bernet,⁴² D. Berninghoff,¹² E. Bertholet,⁸ A. Bertolin,²³ C. Betancourt,⁴² F. Betti,¹⁵ M.-O. Bettler,⁴⁰ M. van Beuzekom,⁴³ I. Bezshyiko,⁴² S. Bifani,⁴⁷ P. Billoir,⁸ A. Birnkraut,¹⁰ A. Bizzeti,^{18,e} M. Bjørn,⁵⁷ T. Blake,⁵⁰ F. Blanc,⁴¹ S. Blusk,⁶¹ V. Bocci,²⁶ T. Boettcher,⁵⁸ A. Bondar,^{36,f} N. Bondar,³¹ I. Bordyuzhin,³² S. Borghi,⁵⁶ M. Borisyak,³⁵ M. Borsato,³⁹ F. Bossu,⁷ M. Boubdir,⁹ T. J. V. Bowcock,⁵⁴ E. Bowen,⁴² C. Bozzi,^{17,40} S. Braun,¹² T. Britton,⁶¹ J. Brodzicka,²⁷ D. Brundu,¹⁶ E. Buchanan,⁴⁸ C. Burr,⁵⁶ A. Bursche,^{16,g} J. Buytaert,⁴⁰ W. Byczynski,⁴⁰ S. Cadeddu,¹⁶ H. Cai,⁶⁴ R. Calabrese,^{17,a} R. Calladine,⁴⁷ M. Calvi,^{21,d} M. Calvo Gomez,^{38,b} A. Camboni,^{38,b} P. Campana,¹⁹ D. H. Campora Perez,⁴⁰ L. Capriotti,⁵⁶ A. Carbone,^{15,h} G. Carboni,^{25,i} R. Cardinale,^{20,j} A. Cardini,¹⁶ P. Carniti,^{21,d} L. Carson,⁵² K. Carvalho Akiba,² G. Casse,⁵⁴ L. Cassina,²¹ M. Cattaneo,⁴⁰ G. Cavallero,^{20,40,j} R. Cenci,^{24,k} D. Chamont,⁷ M. G. Chapman,⁴⁸ M. Charles,⁸ Ph. Charpentier,⁴⁰ G. Chatzikonstantinidis,⁴⁷ M. Chefdeville,⁴ S. Chen,¹⁶ S. F. Cheung,⁵⁷ S.-G. Chitic,⁴⁰ V. Chobanova,^{39,40} M. Chrzaszcz,^{42,27} A. Chubykin,³¹ P. Ciambone,¹⁹ X. Cid Vidal,³⁹ G. Ciezarek,⁴³ P. E. L. Clarke,⁵² M. Clemencic,⁴⁰ H. V. Cliff,⁴⁹ J. Closier,⁴⁰ J. Cogan,⁶ E. Cogneras,⁵ V. Cogoni,^{16,g} L. Cojocariu,³⁰ P. Collins,⁴⁰ T. Colombo,⁴⁰ A. Comerma-Montells,¹² A. Contu,⁴⁰ A. Cook,⁴⁸ G. Coombs,⁴⁰ S. Coquereau,³⁸ G. Corti,⁴⁰ M. Corvo,^{17,a} C. M. Costa Sobral,⁵⁰ B. Couturier,⁴⁰ G. A. Cowan,⁵² D. C. Craik,⁵⁸ A. Crocombe,⁵⁰ M. Cruz Torres,¹ R. Currie,⁵² C. D'Ambrosio,⁴⁰ F. Da Cunha Marinho,² E. Dall'Occo,⁴³ J. Dalseno,⁴⁸ A. Davis,³ O. De Aguiar Francisco,⁴⁰ S. De Capua,⁵⁶ M. De Cian,¹² J. M. De Miranda,¹ L. De Paula,² M. De Serio,^{14,l} P. De Simone,¹⁹ C. T. Dean,⁵³ D. Decamp,⁴ L. Del Buono,⁸ H.-P. Dembinski,¹¹ M. Demmer,¹⁰ A. Dendek,²⁸ D. Derkach,³⁵ O. Deschamps,⁵ F. Dettori,⁵⁴ B. Dey,⁶⁵ A. Di Canto,⁴⁰ P. Di Nezza,¹⁹ H. Dijkstra,⁴⁰ F. Dordei,⁴⁰ M. Dorigo,⁴⁰ A. Dosil Suárez,³⁹ L. Douglas,⁵³ A. Dovbnya,⁴⁵ K. Dreimanis,⁵⁴ L. Dufour,⁴³ G. Dujany,⁸ P. Durante,⁴⁰ R. Dzhelyadin,³⁷ M. Dziewiecki,¹² A. Dziurda,⁴⁰ A. Dzyuba,³¹ S. Easo,⁵¹ M. Ebert,⁵² U. Egede,⁵⁵ V. Egorychev,³² S. Eidelman,^{36,f} S. Eisenhardt,⁵² U. Eitschberger,¹⁰ R. Ekelhof,¹⁰ L. Eklund,⁵³ S. Ely,⁶¹ S. Esen,¹² H. M. Evans,⁴⁹ T. Evans,⁵⁷ A. Falabella,¹⁵ N. Farley,⁴⁷ S. Farry,⁵⁴ D. Fazzini,^{21,d} L. Federici,²⁵ D. Ferguson,⁵² G. Fernandez,³⁸ P. Fernandez Declara,⁴⁰ A. Fernandez Prieto,³⁹ F. Ferrari,¹⁵ F. Ferreira Rodrigues,² M. Ferro-Luzzi,⁴⁰ S. Filippov,³⁴ R. A. Fini,¹⁴ M. Fiorini,^{17,a} M. Firlej,²⁸ C. Fitzpatrick,⁴¹ T. Fiutowski,²⁸ F. Fleuret,^{7,c} K. Fohl,⁴⁰ M. Fontana,^{16,40} F. Fontanelli,^{20,j} D. C. Forshaw,⁶¹ R. Forty,⁴⁰ V. Franco Lima,⁵⁴ M. Frank,⁴⁰ C. Frei,⁴⁰ J. Fu,^{22,m} W. Funk,⁴⁰ E. Furfaro,^{25,i} C. Färber,⁴⁰ E. Gabriel,⁵² A. Gallas Torreira,³⁹ D. Galli,^{15,h} S. Gallorini,²³ S. Gambetta,⁵² M. Gandelman,² P. Gandini,²² Y. Gao,³ L. M. Garcia Martin,⁷⁰ J. García Pardiñas,³⁹ J. Garra Tico,⁴⁹ L. Garrido,³⁸ P. J. Garsed,⁴⁹ D. Gascon,³⁸ C. Gaspar,⁴⁰ L. Gavardi,¹⁰ G. Gazzoni,⁵ D. Gerick,¹² E. Gersabeck,⁵⁶ M. Gersabeck,⁵⁶ T. Gershon,⁵⁰ Ph. Ghez,⁴ S. Gianì,⁴¹ V. Gibson,⁴⁹ O. G. Girard,⁴¹ L. Giubega,³⁰ K. Gizdov,⁵² V. V. Gligorov,⁸ D. Golubkov,³² A. Golutvin,⁵⁵ A. Gomes,^{1,n} I. V. Gorelov,³³ C. Gotti,^{21,d} E. Govorkova,⁴³ J. P. Grabowski,¹² R. Graciani Diaz,³⁸ L. A. Granado Cardoso,⁴⁰ E. Graugés,³⁸ E. Graverini,⁴² G. Graziani,¹⁸ A. Grecu,³⁰ R. Greim,⁹ P. Griffith,¹⁶ L. Grillo,²¹ L. Gruber,⁴⁰ B. R. Gruber Cazon,⁵⁷ O. Grünberg,⁶⁷ E. Gushchin,³⁴ Yu. Guz,³⁷ T. Gys,¹² C. Göbel,⁶² T. Hadavizadeh,⁵⁷ C. Hadjivasiliou,⁵ G. Haefeli,⁴¹ C. Haen,⁴⁰ S. C. Haines,⁴⁹ B. Hamilton,⁶⁰ X. Han,¹² T. H. Hancock,⁵⁷ S. Hansmann-Menzemer,¹² N. Harnew,⁵⁷ S. T. Harnew,⁴⁸ C. Hasse,⁴⁰ M. Hatch,⁴⁰ J. He,⁶³ M. Hecker,⁵⁵ K. Heinicke,¹⁰ A. Heister,⁹ K. Hennessy,⁵⁴ P. Henrard,⁵ L. Henry,⁷⁰ E. van Herwijnen,⁴⁰ M. Heß,⁶⁷ A. Hicheur,² D. Hill,⁵⁷

C. Hombach,⁵⁶ P. H. Hopchev,⁴¹ W. Hu,⁶⁵ Z. C. Huard,⁵⁹ W. Hulsbergen,⁴³ T. Humair,⁵⁵ M. Hushchyn,³⁵ D. Hutchcroft,⁵⁴ P. Ibis,¹⁰ M. Idzik,²⁸ P. Ilten,⁵⁸ R. Jacobsson,⁴⁰ J. Jalocha,⁵⁷ E. Jans,⁴³ A. Jawahery,⁶⁰ F. Jiang,³ M. John,⁵⁷ D. Johnson,⁴⁰ C. R. Jones,⁴⁹ C. Joram,⁴⁰ B. Jost,⁴⁰ N. Jurik,⁵⁷ S. Kandybei,⁴⁵ M. Karacson,⁴⁰ J. M. Kariuki,⁴⁸ S. Karodia,⁵³ N. Kazeev,³⁵ M. Kecke,¹² F. Keizer,⁴⁹ M. Kelsey,⁶¹ M. Kenzie,⁴⁹ T. Ketel,⁴⁴ E. Khairullin,³⁵ B. Khanji,¹² C. Khurewathanakul,⁴¹ T. Kirn,⁹ S. Klaver,⁵⁶ K. Klimaszewski,²⁹ T. Klimkovich,¹¹ S. Koliiev,⁴⁶ M. Kolpin,¹² R. Kopecna,¹² P. Koppenburg,⁴³ A. Kosmyntseva,³² S. Kotriakhova,³¹ M. Kozeiha,⁵ L. Kravchuk,³⁴ M. Kreps,⁵⁰ F. Kress,⁵⁵ P. Krokovny,^{36,f} F. Kruse,¹⁰ W. Krzemien,²⁹ W. Kucewicz,^{27,o} M. Kucharczyk,²⁷ V. Kudryavtsev,^{36,f} A. K. Kuonen,⁴¹ T. Kvaratskheliya,^{32,40} D. Lacarrere,⁴⁰ G. Lafferty,⁵⁶ A. Lai,¹⁶ G. Lanfranchi,¹⁹ C. Langenbruch,⁹ T. Latham,⁵⁰ C. Lazzeroni,⁴⁷ R. Le Gac,⁶ A. Leflat,^{33,40} J. Lefrançois,⁷ R. Lefèvre,⁵ F. Lemaître,⁴⁰ E. Lemos Cid,³⁹ O. Leroy,⁶ T. Lesiak,²⁷ B. Leverington,¹² P.-R. Li,⁶³ T. Li,³ Y. Li,⁷ Z. Li,⁶¹ T. Likhomanenko,⁶⁸ R. Lindner,⁴⁰ F. Lionetto,⁴² V. Lisovskyi,⁷ X. Liu,³ D. Loh,⁵⁰ A. Loi,¹⁶ I. Longstaff,⁵³ J. H. Lopes,² D. Lucchesi,^{23,p} M. Lucio Martinez,³⁹ H. Luo,⁵² A. Lupato,²³ E. Luppi,^{17,a} O. Lupton,⁴⁰ A. Lusiani,²⁴ X. Lyu,⁶³ F. Machefert,⁷ F. Maciuc,³⁰ V. Macko,⁴¹ P. Mackowiak,¹⁰ S. Maddrell-Mander,⁴⁸ O. Maev,^{31,40} K. Maguire,⁵⁶ D. Maisuzenko,³¹ M. W. Majewski,²⁸ S. Malde,⁵⁷ B. Malecki,²⁷ A. Malinin,⁶⁸ T. Maltsev,^{36,f} G. Manca,^{16,g} G. Mancinelli,⁶ D. Marangotto,^{22,m} J. Maratas,^{5,q} J. F. Marchand,⁴ U. Marconi,¹⁵ C. Marin Benito,³⁸ M. Marinangeli,⁴¹ P. Marino,⁴¹ J. Marks,¹² G. Martellotti,²⁶ M. Martin,⁶ M. Martinelli,⁴¹ D. Martinez Santos,³⁹ F. Martinez Vidal,⁷⁰ L. M. Massacrier,⁷ A. Massafferri,¹ R. Matev,⁴⁰ A. Mathad,⁵⁰ Z. Mathe,⁴⁰ C. Matteuzzi,²¹ A. Mauri,⁴² E. Maurice,^{7,c} B. Maurin,⁴¹ A. Mazurov,⁴⁷ M. McCann,^{55,40} A. McNab,⁵⁶ R. McNulty,¹³ J. V. Mead,⁵⁴ B. Meadows,⁵⁹ C. Meaux,⁶ F. Meier,¹⁰ N. Meinert,⁶⁷ D. Melnychuk,²⁹ M. Merk,⁴³ A. Merli,^{22,40,m} E. Michielin,²³ D. A. Milanes,⁶⁶ E. Millard,⁵⁰ M.-N. Minard,⁴ L. Minzoni,¹⁷ D. S. Mitzel,¹² A. Mogini,⁸ J. Molina Rodriguez,¹ T. Mombächer,¹⁰ I. A. Monroy,⁶⁶ S. Monteil,⁵ M. Morandin,²³ M. J. Morello,^{24,k} O. Morgunova,⁶⁸ J. Moron,²⁸ A. B. Morris,⁵² R. Mountain,⁶¹ F. Muheim,⁵² M. Mulder,⁴³ D. Müller,⁵⁶ J. Müller,¹⁰ K. Müller,⁴² V. Müller,¹⁰ P. Naik,⁴⁸ T. Nakada,⁴¹ R. Nandakumar,⁵¹ A. Nandi,⁵⁷ I. Nasteva,² M. Needham,⁵² N. Neri,^{22,40} S. Neubert,¹² N. Neufeld,⁴⁰ M. Neuner,¹² T. D. Nguyen,⁴¹ C. Nguyen-Mau,^{41,r} S. Nieswand,⁹ R. Niet,¹⁰ N. Nikitin,³³ T. Nikodem,¹² A. Nogay,⁶⁸ D. P. O'Hanlon,⁵⁰ A. Oblakowska-Mucha,²⁸ V. Obraztsov,³⁷ S. Ogilvy,¹⁹ R. Oldeman,^{16,g} C. J. G. Onderwater,⁷¹ A. Ossowska,²⁷ J. M. Otalora Goicochea,² P. Owen,⁴² A. Oyanguren,⁷⁰ P. R. Pais,⁴¹ A. Palano,¹⁴ M. Palutan,^{19,40} A. Papanestis,⁵¹ M. Pappagallo,^{14,l} L. L. Pappalardo,^{17,a} W. Parker,⁶⁰ C. Parkes,⁵⁶ G. Passaleva,^{18,40} A. Pastore,^{14,l} M. Patel,⁵⁵ C. Patrignani,^{15,h} A. Pearce,⁴⁰ A. Pellegrino,⁴³ G. Penso,²⁶ M. Pepe Altarelli,⁴⁰ S. Perazzini,⁴⁰ P. Perret,⁵ L. Pescatore,⁴¹ K. Petridis,⁴⁸ A. Petrolini,^{20,j} A. Petrov,⁶⁸ M. Petruzzo,^{22,m} E. Picatoste Olloqui,³⁸ B. Pietrzyk,⁴ M. Pikies,²⁷ D. Pinci,²⁶ F. Pisani,⁴⁰ A. Pistone,^{20,j} A. Piucci,¹² V. Placinta,³⁰ S. Playfer,⁵² M. Plo Casasus,³⁹ F. Polci,⁸ M. Poli Lener,¹⁹ A. Poluektov,⁵⁰ I. Polyakov,⁶¹ E. Polycarpo,² G. J. Pomery,⁴⁸ S. Ponce,⁴⁰ A. Popov,³⁷ D. Popov,^{11,40} S. Poslavskii,³⁷ C. Potterat,² E. Price,⁴⁸ J. Prisciandaro,³⁹ C. Prouve,⁴⁸ V. Pugatch,⁴⁶ A. Puig Navarro,⁴² H. Pullen,⁵⁷ G. Punzi,^{24,s} W. Qian,⁵⁰ R. Quagliani,^{7,48} B. Quintana,⁵ B. Rachwal,²⁸ J. H. Rademacker,⁴⁸ M. Rama,²⁴ M. Ramos Pernas,³⁹ M. S. Rangel,² I. Raniuk,^{45,†} F. Ratnikov,³⁵ G. Raven,⁴⁴ M. Ravonel Salzgeber,⁴⁰ M. Reboud,⁴ F. Redi,⁵⁵ S. Reichert,¹⁰ A. C. dos Reis,¹ C. Remon Alepuz,⁷⁰ V. Renaudin,⁷ S. Ricciardi,⁵¹ S. Richards,⁴⁸ M. Rihl,⁴⁰ K. Rinnert,⁵⁴ V. Rives Molina,³⁸ P. Robbe,⁷ A. Robert,⁸ A. B. Rodrigues,¹ E. Rodrigues,⁵⁹ J. A. Rodriguez Lopez,⁶⁶ A. Rogozhnikov,³⁵ S. Roiser,⁴⁰ A. Rollings,⁵⁷ V. Romanovskiy,³⁷ A. Romero Vidal,³⁹ J. W. Ronayne,¹³ M. Rotondo,¹⁹ M. S. Rudolph,⁶¹ T. Ruf,⁴⁰ P. Ruiz Valls,⁷⁰ J. Ruiz Vidal,⁷⁰ J. J. Saborido Silva,³⁹ E. Sadykhov,³² N. Sagidova,³¹ B. Saitta,^{16,g} V. Salustino Guimaraes,⁶² C. Sanchez Mayordomo,⁷⁰ B. Sanmartin Sedes,³⁹ R. Santacesaria,²⁶ C. Santamarina Rios,³⁹ M. Santimaria,¹⁹ E. Santovetti,^{25,i} G. Sarpis,⁵⁶ A. Sarti,^{19,t} C. Satriano,^{26,u} A. Satta,²⁵ D. M. Saunders,⁴⁸ D. Savrina,^{32,33} S. Schael,⁹ M. Schellenberg,¹⁰ M. Schiller,⁵³ H. Schindler,⁴⁰ M. Schmelling,¹¹ T. Schmelzer,¹⁰ B. Schmidt,⁴⁰ O. Schneider,⁴¹ A. Schopper,⁴⁰ H. F. Schreiner,⁵⁹ M. Schubiger,⁴¹ M.-H. Schune,⁷ R. Schwemmer,⁴⁰ B. Sciascia,¹⁹ A. Sciubba,^{26,t} A. Semennikov,³² E. S. Sepulveda,⁸ A. Sergi,⁴⁷ N. Serra,⁴² J. Serrano,⁶ L. Sestini,²³ P. Seyfert,⁴⁰ M. Shapkin,³⁷ I. Shapoval,⁴⁵ Y. Shcheglov,³¹ T. Shears,⁵⁴ L. Shekhtman,^{36,f} V. Shevchenko,⁶⁸ B. G. Siddi,¹⁷ R. Silva Coutinho,⁴² L. Silva de Oliveira,² G. Simi,^{23,p} S. Simone,^{14,l} M. Sirendi,⁴⁹ N. Skidmore,⁴⁸ T. Skwarnicki,⁶¹ E. Smith,⁵⁵ I. T. Smith,⁵² J. Smith,⁴⁹ M. Smith,⁵⁵ I. Soares Lavra,¹ M. D. Sokoloff,⁵⁹ F. J. P. Soler,⁵³ B. Souza De Paula,² B. Spaan,¹⁰ P. Spradlin,⁵³ S. Sridharan,⁴⁰ F. Stagni,⁴⁰ M. Stahl,¹² S. Stahl,⁴⁰ P. Stefko,⁴¹ S. Stefkova,⁵⁵ O. Steinkamp,⁴² S. Stemmler,¹² O. Stenyakin,³⁷ M. Stepanova,³¹ H. Stevens,¹⁰ S. Stone,⁶¹ B. Storaci,⁴² S. Stracka,^{24,s} M. E. Stramaglia,⁴¹ M. Straticiu,³⁰ U. Straumann,⁴² J. Sun,³ L. Sun,⁶⁴ W. Sutcliffe,⁵⁵ K. Swientek,²⁸ V. Syropoulos,⁴⁴ T. Szumlak,²⁸ M. Szymanski,⁶³ S. T'Jampens,⁴ A. Tayduganov,⁶ T. Tekampe,¹⁰ G. Tellarini,^{17,a} F. Teubert,⁴⁰ E. Thomas,⁴⁰ J. van Tilburg,⁴³ M. J. Tilley,⁵⁵ V. Tisserand,⁴ M. Tobin,⁴¹ S. Tolk,⁴⁹ L. Tomassetti,^{17,a}

D. Tonelli,²⁴ F. Toriello,⁶¹ R. Tourinho Jadallah Aoude,¹ E. Tournefier,⁴ M. Traill,⁵³ M. T. Tran,⁴¹ M. Tresch,⁴² A. Trisovic,⁴⁰ A. Tsaregorodtsev,⁶ P. Tsopelas,⁴³ A. Tully,⁴⁹ N. Tuning,^{43,40} A. Ukleja,²⁹ A. Usachov,⁷ A. Ustyuzhanin,³⁵ U. Uwer,¹² C. Vacca,^{16,g} A. Vagner,⁶⁹ V. Vagnoni,^{15,40} A. Valassi,⁴⁰ S. Valat,⁴⁰ G. Valenti,¹⁵ R. Vazquez Gomez,⁴⁰ P. Vazquez Regueiro,³⁹ S. Vecchi,¹⁷ M. van Veghel,⁴³ J. J. Velthuis,⁴⁸ M. Veltri,^{18,v} G. Veneziano,⁵⁷ A. Venkateswaran,⁶¹ T. A. Verlage,⁹ M. Vernet,⁵ M. Vesterinen,⁵⁷ J. V. Viana Barbosa,⁴⁰ B. Viaud,⁷ D. Vieira,⁶³ M. Vieites Diaz,³⁹ H. Viemann,⁶⁷ X. Vilasis-Cardona,^{38,b} M. Vitti,⁴⁹ V. Volkov,³³ A. Vollhardt,⁴² B. Voneki,⁴⁰ A. Vorobyev,³¹ V. Vorobyev,^{36,f} C. Voß,⁹ J. A. de Vries,⁴³ C. Vázquez Sierra,³⁹ R. Waldi,⁶⁷ C. Wallace,⁵⁰ R. Wallace,¹³ J. Walsh,²⁴ J. Wang,⁶¹ D. R. Ward,⁴⁹ H. M. Wark,⁵⁴ N. K. Watson,⁴⁷ D. Websdale,⁵⁵ A. Weiden,⁴² C. Weisser,⁵⁸ M. Whitehead,⁴⁰ J. Wicht,⁵⁰ G. Wilkinson,⁵⁷ M. Wilkinson,⁶¹ M. Williams,⁵⁶ M. P. Williams,⁴⁷ M. Williams,⁵⁸ T. Williams,⁴⁷ F. F. Wilson,^{51,40} J. Wimberley,⁶⁰ M. Winn,⁷ J. Wishahi,¹⁰ W. Wislicki,²⁹ M. Witek,²⁷ G. Wormser,⁷ S. A. Wotton,⁴⁹ K. Wraight,⁵³ K. Wyllie,⁴⁰ Y. Xie,⁶⁵ M. Xu,⁶⁵ Z. Xu,⁴ Z. Yang,³ Z. Yang,⁶⁰ Y. Yao,⁶¹ H. Yin,⁶⁵ J. Yu,⁶⁵ X. Yuan,⁶¹ O. Yushchenko,³⁷ K. A. Zarebski,⁴⁷ M. Zavertyaev,^{11,w} L. Zhang,³ Y. Zhang,⁷ A. Zhelezov,¹² Y. Zheng,⁶³ X. Zhu,³ V. Zhukov,³³ J. B. Zonneveld,⁵² and S. Zucchelli¹⁵

(LHCb Collaboration)

¹Centro Brasileiro de Pesquisas Físicas (CBPF), Rio de Janeiro, Brazil

²Universidade Federal do Rio de Janeiro (UFRJ), Rio de Janeiro, Brazil

³Center for High Energy Physics, Tsinghua University, Beijing, China

⁴LAPP, Université Savoie Mont-Blanc, CNRS/IN2P3, Annecy-Le-Vieux, France

⁵Clermont Université, Université Blaise Pascal, CNRS/IN2P3, LPC, Clermont-Ferrand, France

⁶Aix Marseille Université, CNRS/IN2P3, CPPM, Marseille, France

⁷LAL, Université Paris-Sud, CNRS/IN2P3, Orsay, France

⁸LPNHE, Université Pierre et Marie Curie, Université Paris Diderot, CNRS/IN2P3, Paris, France

⁹I. Physikalisches Institut, RWTH Aachen University, Aachen, Germany

¹⁰Fakultät Physik, Technische Universität Dortmund, Dortmund, Germany

¹¹Max-Planck-Institut für Kernphysik (MPIK), Heidelberg, Germany

¹²Physikalisches Institut, Ruprecht-Karls-Universität Heidelberg, Heidelberg, Germany

¹³School of Physics, University College Dublin, Dublin, Ireland

¹⁴Sezione INFN di Bari, Bari, Italy

¹⁵Sezione INFN di Bologna, Bologna, Italy

¹⁶Sezione INFN di Cagliari, Cagliari, Italy

¹⁷Università e INFN, Ferrara, Ferrara, Italy

¹⁸Sezione INFN di Firenze, Firenze, Italy

¹⁹Laboratori Nazionali dell'INFN di Frascati, Frascati, Italy

²⁰Sezione INFN di Genova, Genova, Italy

²¹Università e INFN, Milano-Bicocca, Milano, Italy

²²Sezione di Milano, Milano, Italy

²³Sezione INFN di Padova, Padova, Italy

²⁴Sezione INFN di Pisa, Pisa, Italy

²⁵Sezione INFN di Roma Tor Vergata, Roma, Italy

²⁶Sezione INFN di Roma La Sapienza, Roma, Italy

²⁷Henryk Niewodniczanski Institute of Nuclear Physics Polish Academy of Sciences, Kraków, Poland

²⁸AGH—University of Science and Technology, Faculty of Physics and Applied Computer Science, Kraków, Poland

²⁹National Center for Nuclear Research (NCBJ), Warsaw, Poland

³⁰Horia Hulubei National Institute of Physics and Nuclear Engineering, Bucharest-Magurele, Romania

³¹Petersburg Nuclear Physics Institute (PNPI), Gatchina, Russia

³²Institute of Theoretical and Experimental Physics (ITEP), Moscow, Russia

³³Institute of Nuclear Physics, Moscow State University (SINP MSU), Moscow, Russia

³⁴Institute for Nuclear Research of the Russian Academy of Sciences (INR RAN), Moscow, Russia

³⁵Yandex School of Data Analysis, Moscow, Russia

³⁶Budker Institute of Nuclear Physics (SB RAS), Novosibirsk, Russia

³⁷Institute for High Energy Physics (IHEP), Protvino, Russia

³⁸ICCUB, Universitat de Barcelona, Barcelona, Spain

³⁹Universidad de Santiago de Compostela, Santiago de Compostela, Spain

⁴⁰European Organization for Nuclear Research (CERN), Geneva, Switzerland

⁴¹Institute of Physics, Ecole Polytechnique Fédérale de Lausanne (EPFL), Lausanne, Switzerland

- ⁴²*Physik-Institut, Universität Zürich, Zürich, Switzerland*
- ⁴³*Nikhef National Institute for Subatomic Physics, Amsterdam, The Netherlands*
- ⁴⁴*Nikhef National Institute for Subatomic Physics and VU University Amsterdam, Amsterdam, The Netherlands*
- ⁴⁵*NSC Kharkiv Institute of Physics and Technology (NSC KIPT), Kharkiv, Ukraine*
- ⁴⁶*Institute for Nuclear Research of the National Academy of Sciences (KINR), Kyiv, Ukraine*
- ⁴⁷*University of Birmingham, Birmingham, United Kingdom*
- ⁴⁸*H.H. Wills Physics Laboratory, University of Bristol, Bristol, United Kingdom*
- ⁴⁹*Cavendish Laboratory, University of Cambridge, Cambridge, United Kingdom*
- ⁵⁰*Department of Physics, University of Warwick, Coventry, United Kingdom*
- ⁵¹*STFC Rutherford Appleton Laboratory, Didcot, United Kingdom*
- ⁵²*School of Physics and Astronomy, University of Edinburgh, Edinburgh, United Kingdom*
- ⁵³*School of Physics and Astronomy, University of Glasgow, Glasgow, United Kingdom*
- ⁵⁴*Oliver Lodge Laboratory, University of Liverpool, Liverpool, United Kingdom*
- ⁵⁵*Imperial College London, London, United Kingdom*
- ⁵⁶*School of Physics and Astronomy, University of Manchester, Manchester, United Kingdom*
- ⁵⁷*Department of Physics, University of Oxford, Oxford, United Kingdom*
- ⁵⁸*Massachusetts Institute of Technology, Cambridge, Massachusetts, USA*
- ⁵⁹*University of Cincinnati, Cincinnati, Ohio, USA*
- ⁶⁰*University of Maryland, College Park, Maryland, USA*
- ⁶¹*Syracuse University, Syracuse, New York, USA*
- ⁶²*Pontifícia Universidade Católica do Rio de Janeiro (PUC-Rio), Rio de Janeiro, Brazil*
(associated with Institution Universidade Federal do Rio de Janeiro (UFRJ), Rio de Janeiro, Brazil)
- ⁶³*University of Chinese Academy of Sciences, Beijing, China*
(associated with Institution Center for High Energy Physics, Tsinghua University, Beijing, China)
- ⁶⁴*School of Physics and Technology, Wuhan University, Wuhan, China*
(associated with Institution Center for High Energy Physics, Tsinghua University, Beijing, China)
- ⁶⁵*Institute of Particle Physics, Central China Normal University, Wuhan, Hubei, China*
(associated with Institution Center for High Energy Physics, Tsinghua University, Beijing, China)
- ⁶⁶*Departamento de Física, Universidad Nacional de Colombia, Bogota, Colombia*
(associated with Institution LPNHE, Université Pierre et Marie Curie, Université Paris Diderot, CNRS/IN2P3, Paris, France)
- ⁶⁷*Institut für Physik, Universität Rostock, Rostock, Germany*
(associated with Institution Physikalisches Institut, Ruprecht-Karls-Universität Heidelberg, Heidelberg, Germany)
- ⁶⁸*National Research Centre Kurchatov Institute, Moscow, Russia*
(associated with Institution Institute of Theoretical and Experimental Physics (ITEP), Moscow, Russia)
- ⁶⁹*National Research Tomsk Polytechnic University, Tomsk, Russia*
(associated with Institution Institute of Theoretical and Experimental Physics (ITEP), Moscow, Russia)
- ⁷⁰*Instituto de Física Corpuscular, Centro Mixto Universidad de Valencia—CSIC, Valencia, Spain*
(associated with Institution ICCUB, Universitat de Barcelona, Barcelona, Spain)
- ⁷¹*Van Swinderen Institute, University of Groningen, Groningen, The Netherlands*
(associated with Institution Nikhef National Institute for Subatomic Physics, Amsterdam, The Netherlands)

[†]Deceased.

^aAlso at Università di Ferrara, Ferrara, Italy.

^bAlso at LIFAELS, La Salle, Universitat Ramon Llull, Barcelona, Spain.

^cAlso at Laboratoire Leprince-Ringuet, Palaiseau, France.

^dAlso at Università di Milano Bicocca, Milano, Italy.

^eAlso at Università di Modena e Reggio Emilia, Modena, Italy.

^fAlso at Novosibirsk State University, Novosibirsk, Russia.

^gAlso at Università di Cagliari, Cagliari, Italy.

^hAlso at Università di Bologna, Bologna, Italy.

ⁱAlso at Università di Roma Tor Vergata, Roma, Italy.

^jAlso at Università di Genova, Genova, Italy.

^kAlso at Scuola Normale Superiore, Pisa, Italy.

^lAlso at Università di Bari, Bari, Italy.

^mAlso at Università degli Studi di Milano, Milano, Italy.

ⁿAlso at Universidade Federal do Triângulo Mineiro (UFMT), Uberaba-MG, Brazil.

^oAlso at AGH—University of Science and Technology, Faculty of Computer Science, Electronics and Telecommunications, Kraków, Poland.

^pAlso at Università di Padova, Padova, Italy.

^qAlso at Iligan Institute of Technology (IIT), Iligan, Philippines.

^rAlso at Hanoi University of Science, Hanoi, Vietnam.

^sAlso at Università di Pisa, Pisa, Italy.

^tAlso at Università di Roma La Sapienza, Roma, Italy.

^uAlso at Università della Basilicata, Potenza, Italy.

^vAlso at Università di Urbino, Urbino, Italy.

^wAlso at P.N. Lebedev Physical Institute, Russian Academy of Science (LPI RAS), Moscow, Russia.